



Preference of Afternoon Precipitation Over Dry Soil in the North China Plain During Warm Seasons

Sixuan Li¹, Jianping Guo² , Xuanze Zhang³, Bing Tong⁴ , Tianning Su⁵ , Jing Wei⁵, and Zhanqing Li⁵ 

Special Section:

Scientific Impact of Long-term Observations of the Atmosphere - In Honor of Walter Komhyr (1931 - 2022)

Key Points:

- The North China Plain is a strong land-atmosphere coupling area during warm seasons
- In general, afternoon precipitation events (APEs) are more likely to be initiated over dry soil
- However, for more stable and moister atmosphere, APEs are more likely to occur on wet soil

Supporting Information:

Supporting Information may be found in the online version of this article.

Correspondence to:

J. Guo and Z. Li,
jguocams@gmail.com;
zli@atmos.umd.edu

Citation:

Li, S., Guo, J., Zhang, X., Tong, B., Su, T., Wei, J., & Li, Z. (2024). Preference of afternoon precipitation over dry soil in the North China Plain during warm seasons. *Journal of Geophysical Research: Atmospheres*, 129, e2023JD040641. <https://doi.org/10.1029/2023JD040641>

Received 20 DEC 2023
 Accepted 27 MAR 2024

Author Contributions:

Conceptualization: Sixuan Li, Jianping Guo, Zhanqing Li
Data curation: Sixuan Li, Jianping Guo, Xuanze Zhang, Bing Tong, Jing Wei, Zhanqing Li
Formal analysis: Sixuan Li, Jianping Guo
Funding acquisition: Jianping Guo, Zhanqing Li
Investigation: Sixuan Li, Jianping Guo, Xuanze Zhang, Zhanqing Li
Methodology: Sixuan Li, Jianping Guo, Zhanqing Li

© 2024. The Authors.

This is an open access article under the terms of the [Creative Commons Attribution License](https://creativecommons.org/licenses/by/4.0/), which permits use, distribution and reproduction in any medium, provided the original work is properly cited.

¹State Key Laboratory of Remote Sensing Science, Faculty of Geographical Science, Beijing Normal University, Beijing, China, ²State Key Laboratory of Severe Weather, Chinese Academy of Meteorological Sciences, Beijing, China, ³Key Laboratory of Water Cycle and Related Land Surface Processes, Institute of Geographic Sciences and Natural Resources Research, Chinese Academy of Sciences, Beijing, China, ⁴State Key Laboratory of Urban and Regional Ecology, Research Center for Eco-environmental Sciences, Chinese Academy of Sciences, Beijing, China, ⁵Department of Atmospheric and Oceanic Sciences, Earth System Science Interdisciplinary Center, College Park, MD, USA

Abstract The influence of soil moisture (SM) on atmospheric precipitation has been extensively studied, but few of these studies have considered the role of land-atmosphere (L-A) coupling in afternoon precipitation events (APEs) at a sub-daily timescale. Here, using in-situ observations and reanalysis data sets, we investigated the effect of the soil moisture anomaly (SMA) on warm seasons' afternoon precipitation in the North China Plain (NCP), identified as a strong L-A coupling region. APEs were separated from all precipitation events in the NCP during the warm seasons of 2010–2019. It follows from a comparative analysis that an APE is more likely to be initiated on drier soil, which has little dependence on the thresholds used for identifying an APE. However, no affirmative relationship is found between precipitation amount in the first hour of an APE (APE_{1hour}) and the SMA. Further analyses indicate that larger amounts of APE_{1hour} result from higher convective available potential energy (CAPE), higher moist static energy (MSE), or weaker vertical shear of horizontal wind. When considering the joint effects of SMA and atmospheric variables, APEs tend to occur on drier (wetter) soil with lower (higher) lower-tropospheric stability, CAPE, or MSE. This study highlights the significant roles of L-A interactions on local atmospheric precipitation, especially the joint roles of SM and atmospheric variables on precipitation.

Plain Language Summary Atmospheric precipitation events (APEs) are mostly the consequence of atmospheric circulation anomalies and water vapor and energy transport supplies from the atmosphere and land surface. Previous studies have reported the important role of the soil moisture anomaly (SMA) on convective precipitation events, but how SMA influences the subsequent convective precipitation remains highly uncertain. In this work, we focus on the impact of morning SMA on subsequent local-scale afternoon precipitation during warm seasons. Using in-situ observations, we identified the North China Plain as a strong land-atmosphere (L-A) coupling area in China, further finding that warm seasons' APEs tend to occur on dry soil. However, the precipitation amount associated with an APE is almost independent of SMA. A joint analysis indicates that larger precipitation amounts result from higher moist static energy, convective available potential energy, or weaker vertical shear of horizontal wind. This study highlights the significant roles of L-A interactions on local atmospheric precipitation.

1. Introduction

Soil moisture (SM) plays an important role in the land-atmosphere (L-A) system because it determines the exchange of energy, water, and carbon fluxes between the surface and the atmosphere (Eltahir, 1998; Santanello et al., 2018; Seneviratne et al., 2010; Zhang et al., 2023). Through partitioning surface net radiation energy into latent and sensible heat fluxes, SM influences the land surface temperature and the planetary boundary layer (PBL) evolution (Huang et al., 2013; Milovac et al., 2016; Tong et al., 2022), hence cloud formation and afternoon convective precipitation (Findell & Eltahir, 2003a, 2003b; Gentine et al., 2013).

The effects of SM on rainfall have been investigated in different parts of the world (Ferguson et al., 2012; Guillod et al., 2015; Petrova et al., 2018; Taylor et al., 2011). On a global scale, Taylor et al. (2012) found that afternoon rainfall tended to occur over soils that were relatively drier than the surrounding areas. Specifically, Cook et al. (2006) found that higher SM values corresponded to a lower precipitation frequency and amount in Southern

Project administration: Jianping Guo, Zhanqing Li
Resources: Jianping Guo, Zhanqing Li
Software: Sixuan Li
Supervision: Jianping Guo, Zhanqing Li
Validation: Sixuan Li, Jianping Guo, Xuanze Zhang, Bing Tong, Tianning Su, Jing Wei, Zhanqing Li
Visualization: Sixuan Li
Writing – original draft: Sixuan Li
Writing – review & editing: Sixuan Li, Jianping Guo, Xuanze Zhang, Zhanqing Li

Africa. These studies are indicative of a negative SM-rainfall feedback. On the other hand, SM may also have a positive feedback on precipitation. In the eastern U.S. and Mexico, Findell et al. (2011) found that high evaporation over wet soils enhanced the occurrence of afternoon rainfall. Positive correlations were also found between morning SM and subsequent afternoon rainfall amounts when daily water vapor convergence was high in the Southern Great Plains of the U.S. (Welty & Zeng, 2018). The correlation between collocated SM and next-day rainfall amount in northern Australia was also positive (Holgate et al., 2019). In general, how SM influences subsequent precipitation remains uncertain, which can vary considerably from region to region and even at different spatiotemporal scales.

Feedbacks between the land and atmosphere are extremely complex, especially when considering the strong heterogeneity of the land surface (Seneviratne et al., 2010). China is a vast territory with a wide range of climate regimes and diverse land surface types, strongly influenced by the Asian monsoon system, making L-A interactions in China especially complex. The importance of L-A coupling in China has been identified in modeling studies. Dirmeyer (2000) found that accounting for SM in a coupled model significantly improved the simulation of surface temperature and rainfall patterns, especially in monsoonal Asia. Based on multi-model estimations, Koster et al. (2004) further identified North American, the Sahel, India and China as strong L-A coupling regions based on multi-model estimations. Accounting for L-A coupling is important for rainfall prediction in China which is strongly influenced by the Asian monsoon system (Dirmeyer, 2000). Zhong et al. (2018) found that dry soil in East China leads to less precipitation over South China and Central China and more precipitation in East China.

L-A coupling studies have been carried out across a range of spatiotemporal perspectives. Most of the studies related to the effect of SM on precipitation (SM-P) in China are concerned with large-scale coupling, usually associated with non-local effects and long timescale effects (Fan et al., 2019; Liang & Chen, 2010; Ma et al., 2000; Zuo & Zhang, 2007). For example, positive spring SM anomalies over the eastern Tibetan Plateau (TP) lead to more precipitation in the Yangtze River basin (Zhu et al., 2023). There is a positive (negative) correlation between spring SM over the northeastern TP and summer precipitation over North (South) China (Li & Wang, 2016). High SM in the lower and middle reaches of the Yangtze River valley in spring leads to more precipitation over northeastern China in summer and less in southeastern China (Liu et al., 2017; Zuo & Zhang, 2011). However, studies on local-scale SM-P coupling are relatively rare. Local-scale SM-P coupling incorporates the notion that all interactions between land and atmosphere begin locally through the interface of the land surface and the PBL (Santanello et al., 2018). Using a slab model and framework developed by Findell and Eltahir (2003a), Zhao et al. (2022) found a positive feedback in the center of the TP and a negative feedback southwest of the TP between SM and afternoon convection. However, these model results are largely dependent on the parameterization of convection. Previous studies (Gao et al., 2018; Li et al., 2017) have revealed strong L-A coupling in North China based on monthly correlation coefficients of reanalysis data and multi-model ensemble data. However, only a few studies (for example, Talib et al., 2023) have focused on the local impact of SM on afternoon convective precipitation using in-situ observations.

To quantify critical aspects of the L-A system, a series of L-A coupling metrics was developed (Dirmeyer, 2011; Guo et al., 2006; Su et al., 2022; Tawfik & Dirmeyer, 2014). These metrics are statistical and process-based in nature (Santanello et al., 2018; Su et al., 2023). Two-legged metrics are one of the statistical metrics, linking land-surface conditions with atmospheric responses. Two-legged means that the connection from SM to precipitation (P) is separated into two segments: the impact of SM on surface fluxes (terrestrial leg) and the impact of surface fluxes on atmospheric properties (atmospheric leg). The most used multivariate statistic is the correlation analysis. However, if the SM itself changes little, it would not have an impact on atmospheric variables. The terrestrial leg of two-legged metrics considers not only the correlation between SM and surface heat fluxes but also the potential for SM fluctuations to result in large variations in surface fluxes. Therefore, in this study, two-legged metrics were used to determine the strong coupling area in China utilizing long-term in-situ observational data sets.

After identifying the strong L-A coupling area in China, we examined the influence of SM on precipitation frequency and amount in the key area. Given the frequent occurrence of convective precipitation in warm seasons (Gao et al., 2022; Wu et al., 2023) and the large sensitivity of afternoon convection to surface conditions (Dirmeyer & Chen, 2017; Kang, 2016), we focus on the impact of morning SM on subsequent local-scale afternoon precipitation in China during warm seasons. Afternoon precipitation could be substantially affected by local land-

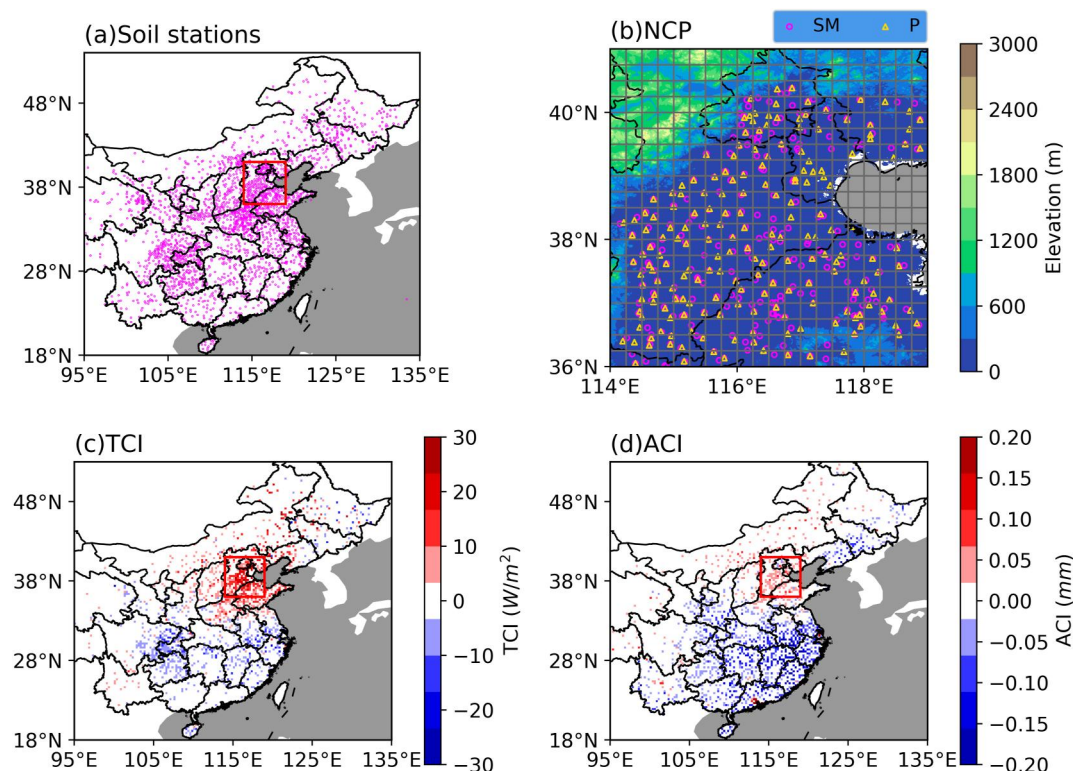


Figure 1. (a) Spatial distribution of soil moisture (SM) stations (pink circles) across China. (b) The zoomed-in map shows SM stations and rain gauge stations (yellow triangles) in the North China Plain with grids at a horizontal resolution of 0.25° longitude \times 0.25° latitude. Terrain elevations are denoted by the background color-shaded area in panel (b). Spatial distributions of (c) the terrestrial coupling index and (d) the atmospheric coupling index in China.

surface coupling processes that influence both evaporation and convection (Guo et al., 2017, 2019; Song & Wei, 2021; Welty & Zeng, 2018). Therefore, to minimize the influence of synoptic-scale forcing, our study focuses on isolated afternoon precipitation events (APEs) occurring between 1400 and 1800 Beijing Time (BJT). We then explored the potential relationship between morning (0800–1200 BJT) SM and afternoon convective precipitation on a sub-daily timescale in the strong coupling area in China to address a basic question: Is afternoon convective precipitation likelier over drier soils or wetter soils? Temporal offsetting of measurements helps isolate the SM forcing of subsequent precipitation. The relationship between SM and afternoon convective precipitation amount was also investigated. Both effects were investigated under different atmospheric conditions because precipitation is driven primarily by atmospheric dynamics and the water vapor supply, while surface and boundary-layer processes also play important roles.

Section 2 describes the data sets used in this study, as well as the calculation of L-A coupling metrics, the strong L-A coupling area in China, and the definition of an APE. In Section 3, the analysis results of the relationship between soil moisture anomaly (SMA) and precipitation frequency and precipitation amount are presented. A summary and discussion are provided in Section 4.

2. Data and Methods

2.1. In Situ Observations

In-situ measurements of volumetric soil water content (Tian et al., 2022) in China during the warm seasons (May–September) of 2010–2019 were adopted for this study. This data set was developed by the China Meteorological Administration (CMA) using Frequency Domain Reflectometry. The volumetric soil water content was observed hourly at 20 evenly spaced layers, ranging from 10 to 200 cm depths, at 2817 meteorological stations across China (Figure 1a), distributed in our study area of 18° – 53° N, 95° – 134° E.

SM influences the land energy and water balance through its impact on evapotranspiration, which includes soil evaporation and plant transpiration (Seneviratne et al., 2010). Through direct evaporation, near-surface SM (0–10 cm) has a significant impact on latent heat flux and thus in triggering convective precipitation (Nicholson, 2015; Petrova et al., 2018). Plant transpiration, which is related to the root-zone SM (10–100 cm), is also an essential driver of surface vapor flux, and transpiration rates depend on plant type and weather. For vegetation-dominated areas in the NCP, changes in root-zone SM generally vary with near-surface SM, which is driven by environmental conditions and vegetation dynamics. Moreover, previous studies have shown that near-surface SM responds to daily and sub-daily time scale weather changes, while root-zone SM, usually associated with land memory, has an impact on persistent atmospheric conditions (Huang & Margulis, 2011; Wetzel et al., 1996). Therefore, in this study, we primarily explore the relationship between near-surface SM and precipitation.

First, the volumetric soil water content during the morning hours (0800–1200 BJT) was averaged at the surface level on each day. Second, the seasonal cycle was removed to calculate SMA. For a given day, SMA was calculated by subtracting the multi-year average SM in that month (Taylor, 2015). SMA was then used to explore the relationship with afternoon precipitation.

Rainfall data used are hourly rainfall amounts from rain gauge measurements made across the NCP during warm seasons for the period of 2010–2019. The station-based measurements were quality controlled and archived by the CMA (Guo et al., 2017). We only retained stations whose elevation is lower than 300 m to filter out precipitation events potentially associated with strong orographic triggers (Guilod et al., 2015; Taylor, 2015). Figure 1b shows the locations of SM stations and rain-gauge stations located at altitudes less than 300 m above mean sea level in the NCP. Finally, we selected 275 SM and 191 precipitation observation sites within the NCP.

Figure 1b also shows that the SM measuring stations are generally not co-located with conventional meteorological stations. The station-based data are gridded at a horizontal resolution of 0.25° longitude \times 0.25° latitude to be consistent with other data sets used (see below). In each grid, the converted gridded mean was computed from all station-based data within the grid (Figure 1b). This spatial averaging also helps lower some random errors in the station-based data (Wang et al., 2022; Xia et al., 2014).

2.2. Reanalysis Data

The Global Land Data Assimilation System (GLDAS) data set is a new generation of reanalysis developed by the National Aeronautics and Space Administration Goddard Space Flight Center and the National Oceanic and Atmospheric Administration National Centers for Environmental Prediction. The GLDAS data set integrates advanced ground- and satellite-based observations to improve the initialization of the forecast model (Rodell et al., 2004). GLDAS version 2.1 is forced with a combination of model and observational meteorological data sets from 2000 to the present, providing various land surface states and fluxes. It has a spatial resolution of $0.25^\circ \times 0.25^\circ$ and a temporal resolution of 3 hr. The SM content of the 0–10 cm soil layer, the sensible heat flux (SHF) and the latent heat flux (LHF) from GLDAS version 2.1 were used in this study. LHF from GLDAS, SM observations, and rain-gauge data from the CMA were used to compute the L-A coupling index. SM data from GLDAS was employed as an alternative data set to validate our findings.

Additional meteorological data are from the fifth-generation European Centre for Medium-Range Weather Forecast (ECMWF) reanalysis (ERA-5), the latest generation of the ECMWF atmospheric reanalysis data set (Hersbach et al., 2020). Benefiting from developments in model physics and data assimilation, ERA-5 has a high resolution of hourly output on a $0.25^\circ \times 0.25^\circ$ horizontal grid. Meteorological variables used in this study include air temperature, specific humidity, height, wind, convective available potential energy (CAPE), and mean vertically integrated moisture divergence (moisture flux divergence (MFD)). Among these variables, air temperature was used to derive lower-tropospheric stability (LTS), which indicates the temperature lapse rate (Klein & Hartmann, 1993). Specific humidity, air temperature, and pressure height were used to derive moist static energy (MSE) (Carey, 1978), which represents the total static energy of the air in the lower atmosphere. Winds at different levels were used to derive the vertical shear of horizontal wind (WSR), representing the dynamic feature of the lower atmosphere. Table 1 summarizes how atmospheric parameters were calculated.

Since we only focus on the antecedent state of afternoon precipitation, SM and other atmospheric variables averaged in the morning hours (0800–1200 BJT) were used in our study.

Table 1
Calculation Method of Atmospheric Parameters for the Precipitation Events

Parameters	Calculation method	Units
WSR (wind shear)	$S = \sqrt{(u_{500mb} - u_{925mb})^2 + (v_{500mb} - v_{925mb})^2}$	m/s
LTS (low-tropospheric stability)	$\Delta\theta = \theta_{700mb} - \theta_{slp}$	K
MSE (moist static energy)	$MSE = C_p T + L_v q + gz$	kJ/kg

Note. θ is potential temperature, T is air temperature, z is geopotential height, q is specific humidity, C_p is the specific heat at constant pressure, L_v is the latent heat of vapourization, g is the gravitational acceleration.

2.3. L-A Coupling Metrics

Following the methods proposed by Dirmeyer (2011), we calculated the terrestrial coupling index (TCI) and the atmospheric coupling index (ACI) of the two-legged metrics as follows:

$$TCI = \sigma_{SM} \frac{\partial LH}{\partial SM} = \frac{\sum(w'_n \times LH'_n)}{\sqrt{N \times \sum(w'_n)^2}}, \quad (1)$$

$$ACI = \sigma_{LH} \frac{\partial P}{\partial LH} = \frac{\sum(LH'_n \times P'_n)}{\sqrt{N \times \sum(LH'_n)^2}}, \quad (2)$$

where in Equation 1, σ_{SM} is the standard deviation of SM, and $\partial LH/\partial SM$ is the linear regression slope, which is a measure of the sensitivity of surface LHF to SM. There are 140×156 grid points in the study area. For each grid point, we estimated TCI using long-term SM and LHF measurements. The anomaly term w'_n is calculated as $w'_n = w_n - \bar{w}$, where w_n denotes the mean SM in the morning hours on a given day n , and \bar{w} denotes the mean SM in the morning hours of all available days at this grid point. The anomaly term LH'_n is calculated as $LH'_n = LH_n - \overline{LH}$, where LH_n denotes LHF on a given day n , and \overline{LH} denotes the temporal mean LHF of all available days at this grid point. N is the number of all available days at a given grid point. ACI is generated in the same way but by substituting the LHF for SM and afternoon precipitation amount for the LHF.

SM influences atmospheric variables through the modification of LHF by evapotranspiration. The sign of TCI can be used to identify the causality between SM and evapotranspiration (Dirmeyer, 2011; Wei & Dirmeyer, 2012). A positive value of TCI indicates that the variation in SM leads to the variation in evapotranspiration. For instance, lower (higher) SM results in less (more) LHF. In extremely arid areas, evapotranspiration responds quickly to SM, but SM varies within a small range, resulting in a low TCI. In humid areas where SM is saturated, the relationship between SM and LHF is poor, resulting in a low TCI. Thus, TCI is generally strong in semi-arid and semi-humid areas. Negative values indicate that the variation in SM is driven by evapotranspiration, which depends on the net solar radiation. Therefore, negative values usually occur when SM is sufficient. A large positive TCI is thus indicative of strong terrestrial coupling with the atmosphere.

To complete the L-A interplay loop, we also calculated ACI, which indicates whether LHF influences precipitation. Similarly, positive values of ACI indicate that the greater the LHF, the heavier the rainfall. Negative values of ACI indicate that the heavier the rainfall, the smaller the LHF. Therefore, L-A hotspots are those regions where both segments of the coupling index are strong.

2.4. Study Area of Strong L-A Coupling

Figures 1c and 1d show the spatial patterns of observation-based TCI and ACI over China from 2010 to 2019. Both show that positive values are mainly distributed in northern China, where the L-A coupling is strong. This is consistent with “hot spots” generated by climate models (Dirmeyer et al., 2014; Koster et al., 2004; Li et al., 2017; Müller et al., 2021; Wei & Dirmeyer, 2012). Positive values of TCI mean that evapotranspiration rates in these areas are sensitive to SM variations, and simultaneously, SM fluctuations could result in large surface flux variations. As the strongest coupling region in China, the NCP is chosen as our target to investigate the influence

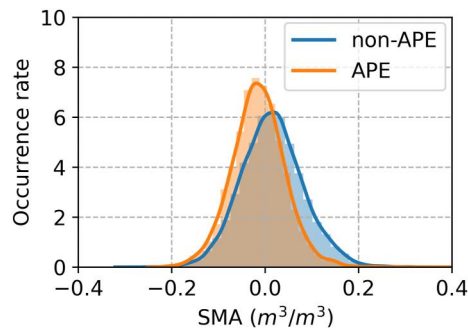


Figure 2. Probability distribution of soil moisture anomaly of “APE” and “non-APE” computed from all rain gauge measurements in the North China Plain.

of surface SM on afternoon precipitation on a sub-daily timescale. By contrast, TCI and ACI are overwhelmingly negative in most parts of southern China, where the surface SM is high during warm seasons. In these regions, evapotranspiration mainly depends on net radiative energy rather than SM (Wei & Dirmeyer, 2012), implying that changes in the boundary layer and consequent convection and precipitation are insensitive to changes in SM in most parts of southern China.

The NCP (36°N–41°N, 114°E–119°E) lies in the semi-humid area of China, bounded by the Yan Mountains to the north, the Taihang Mountains to the west, and the Bohai Sea to the east. Influenced by the East Asia monsoon system (Hu et al., 2017; Wu, 2016), the climate in the NCP is seasonally variable, hot and wet in summer and cold and dry in winter. Precipitation in this region has been found to be sensitive to land surface conditions (Senviratne et al., 2010). In addition, rainfall mainly occurs during the warm seasons in the NCP, which is the period of this study.

2.5. Definition of an APE

First, we selected days when the accumulated precipitation amount during the period 1400–1800 BJT of a given day exceeded 0.3 mm, given that the minimum hourly rainfall is set to 0.1 mm. APEs are defined as isolated rainfall events occurring on days without precipitation recorded on the previous day, the morning of the same day, and the next day. To highlight the potential influence of SM on an APE, we also conducted a comparative analysis between APEs and non-APEs. The constraints of an APE ensure that the relation between antecedent SM and afternoon precipitation is not or minimally affected by large cloud systems with persistent precipitation. Thus, an APE is more likely to be influenced by the state of morning SM and by local thermodynamics. A non-APE may be caused by large-scale synoptic systems, which could affect the state of morning SM. For an APE, the initiation of convection is more influenced by morning SM and pre-storm atmospheric conditions (Zhang et al., 2022). Therefore, the accumulated precipitation in the first hour of a precipitation event (APE_{1hour}) was used to study the influence of morning SM on the precipitation amount of an APE.

3. Results and Discussion

3.1. Afternoon Precipitation and SM

In this section, we mainly focus on the impact of SMA on precipitation frequency. Figure 2 shows that the overall probability density distribution of APE is larger than that of non-APE when SMA is negative. When SMA is positive, the probability of non-APE is higher, indicating that overall, APE tends to occur on drier soil.

From the perspective of spatial distributions, the relationships between APE and SMA in each grid cell were explored. The ratio of days with negative SMA to all available days when precipitation events occurred is calculated in the case of APE and non-APE for each grid cell. Figure 3 reveals that most APEs occur on drier soils (negative correlation), but most non-APEs occur on wetter soils (positive correlation). Moreover, in the NCP, 74.2% of grid boxes for APE (Figure 3a) occur on drier soil, while for non-APE, only 5.5% of grid boxes occur on drier soil (Figure 3b). The results from GLDAS, an alternative SM data set, further corroborate the same tendency for APE on drier soil and non-APE on wetter soil (Figures 3c and 3d).

Surface water and heat fluxes partitioned by SM conditions may influence precipitation by transporting moisture into the atmosphere directly and affecting boundary dynamics indirectly. Moisture recycling (Eltahir, 1998) is expected to lead to a positive correlation, that is, afternoon precipitation is more likely to occur on wetter soil days compared with the mean seasonal cycle. Figures 3b and 3d show that non-APEs occur on wetter soil days (positive correlation), consistent with previous findings of a generally positive correlation for most parts of the world (Findell et al., 2011; Guillod et al., 2015). A positive correlation between SMA and precipitation frequency could be explained by persistent precipitation, which might be induced by synoptic weather systems (Guillod et al., 2014). However, for the isolated APE considered here (i.e., no precipitation on the previous day, the morning of that day, and the next day), we find that an APE

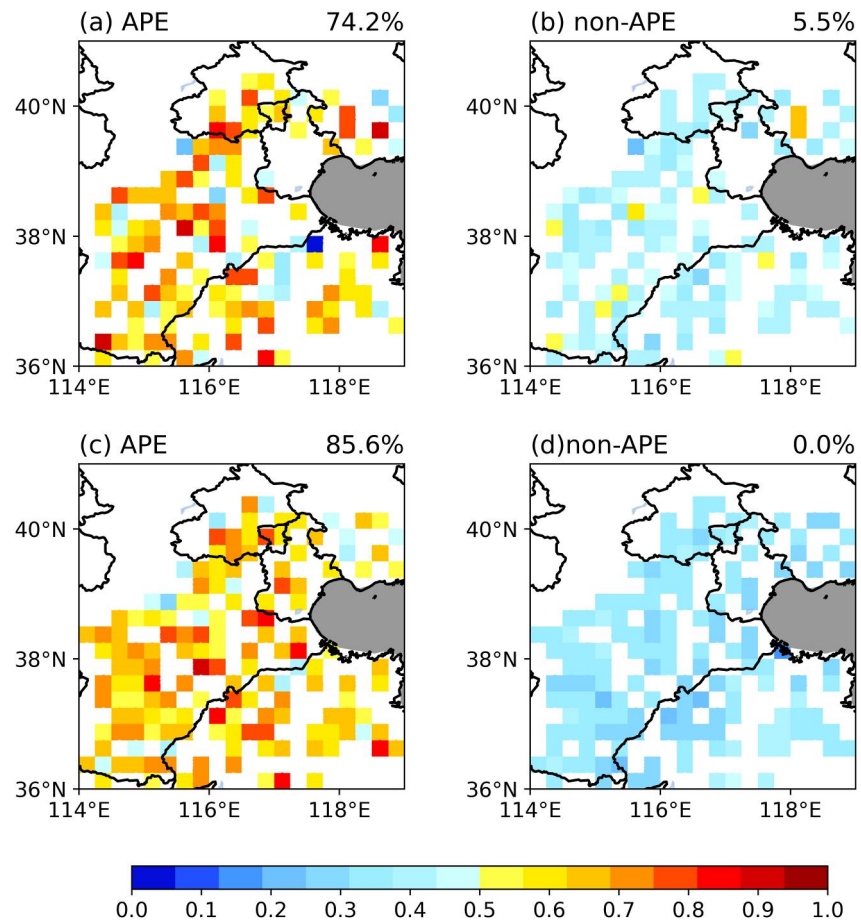


Figure 3. Spatial distribution of the ratio of dry soil moisture (SM) days, which are calculated by in-situ SM observations (a, b) and Global Land Data Assimilation System reanalysis (c, d), to all available rainy days under afternoon precipitation event (APE) (a, c) and non-APE (b, d) conditions. Warm-colored (cool-colored) grid boxes indicate areas where the most precipitation events occur over dry (wet) soil in the morning. The number on the right top corner of each panel represents the percentage of grid points with a ratio that is greater than 0.5.

tends to occur on drier soil in the NCP, indicating a negative correlation. When the average value of SMA for different types of precipitation events is calculated (Figure S1 in Supporting Information S1), APEs again dominate over drier soil, and non-APEs dominate over wetter soil. The negative SMA under APE conditions are stronger than those of SMAs under no-precipitation conditions, indicating that the antecedent SM prior to an APE is even drier than the SM when there is no precipitation in the afternoon. Larger sensible heat fluxes over drier soil than over wetter soil enable air parcels to reach the lifting condensation level (LCL) more readily (Findell & Eltahir, 2003a; Welty et al., 2020). Cloud-resolving models reveal that dry SM yields more vigorous thermals, which can more easily break through the stable layer at the top of the boundary layer, thereby leading to convection and precipitation (Brockhaus et al., 2009). APEs can thus be triggered more readily on days when soil is drier in the morning.

To examine if this finding is subject to the selection of the threshold of minimum accumulated precipitation during 1400–1800 BJT required to determine an APE, we repeated the analysis using different thresholds (Figure 4). Larger thresholds mean a heavier accumulation of precipitation in the afternoon (i.e., 1400–1800 BJT). As the magnitude of the threshold increases, the percentage of grid boxes with APEs over drier soil decreases from 73.4% to 59%, according to observations, and from 85.6% to 63.3%, according to the GLDAS data set. This reinforces our finding that an APE tends to occur over drier soils in the strong L-A coupling region of the NCP, with little regard to the threshold used for identifying afternoon precipitation.

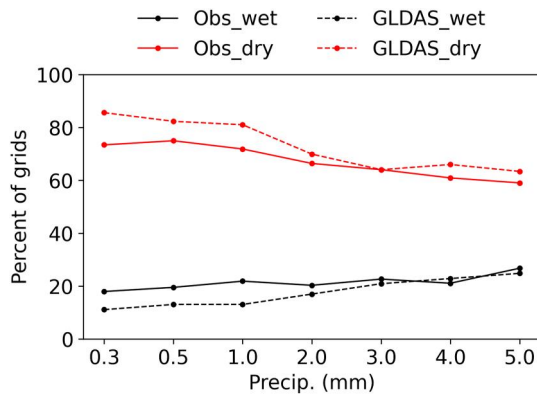


Figure 4. Percentage of grids with afternoon precipitation event in the North China Plain that occur over dry soil (in red) or wet soil (in black) as a function of the threshold of accumulated precipitation amount during the period 1400–1800 Beijing Time, which is calculated using observations (solid lines) and the Global Land Data Assimilation System data set (dashed lines).

3.2. The Relationship Between SMA and Precipitation Amount

In addition to the effect of antecedent SMA on the onset of afternoon precipitation, we also examined the relationship between SMA and afternoon precipitation amount in the first hour of the precipitation event ($APE_{1\text{hour}}$, non- $APE_{1\text{hour}}$). Figure 5 depicts the correlation coefficient (r) for SMA and $APE_{1\text{hour}}$ or non- $APE_{1\text{hour}}$ in each grid cell. The values of r are higher under APE (r : -0.58 – 0.71) than non-APE (r : -0.35 – 0.22) conditions, noting that most values are concentrated around 0 (Figure 5a). Figure 5c shows that r values passing the significance test are negative, most of which are concentrated around -0.2 . Overall, the correlation between SMA and non- $APE_{1\text{hour}}$ is weak, implying that there is almost no relation between SMA and non- $APE_{1\text{hour}}$. On the contrary, positive r values under APE conditions that pass the significance test exceed 0.52 (Figure 5b). There are also negative r values passing the significance test. Although the absolute value of r improved in the case of APE, the sign of r is randomly distributed. The impact of SMA on $APE_{1\text{hour}}$ is thus inconclusive, varying by region. Using the SMA from GLDAS, r is also improved in the case of APE (Figure 6a). Compared with SMA based on observations, most of the r values passing the significance test are positive (10 out of 13 grid boxes, $r > 0.41$, Figure 6b). Results from GLDAS indicate that there might be a prevalent positive correlation under APE conditions, that is, larger $APE_{1\text{hour}}$ values tend to occur over wetter soil.

In summary, $APE_{1\text{hour}}$ is not clearly related to SMA per in-situ observations. However, using the GLDAS SMA, we found a positive correlation between SMA and $APE_{1\text{hour}}$ in the NCP. This is consistent with the finding of Cioni and Hohenegger (2017) who used large-eddy simulations (LES) that the precipitation magnitude is strongly correlated with surface LHF averaged over the duration of precipitation, that is, wetter soils with larger LHF lead to greater precipitation amounts.

The analyses presented in Sections 3.1 and 3.2 reveal a negative correlation between SMA and APE frequency (negative frequency effect), but $APE_{1\text{hour}}$ is not strongly related to SMA. Although the relationship between SMA and $APE_{1\text{hour}}$ is ambiguous according to the in-situ observational data set, a positive correlation emerges from the GLDAS data set (positive intensity effect). Heat flux analyses indicate that both the LHF anomaly (LHFA) and the SHF anomaly (SHFA) in the morning are higher when an APE happens (Figure S2 in Supporting Information S1). Therefore, surface net radiation energy is larger, increasing the possibility of the land surface influencing the evolution of the boundary layer above it and subsequent cloud formation and precipitation. The LHFA is higher on wetter soil than on drier soil, while the SHFA is higher on drier soil than on wetter soil (Figures S3 and S4 in Supporting Information S1). A larger SHFA on drier soil may promote boundary-layer growth, triggering precipitation more readily (negative frequency effect). Wetter soil, which has a larger LHFA, may lead to a greater precipitation amount (positive intensity effect). Although the significant statistical relationship between morning SMA and APE does not necessarily imply a direct SM-P coupling (Holgate et al., 2019), it may serve as a steppingstone toward understanding the physical mechanisms driving L-A coupling.

3.3. The Joint Effect of SM and Atmospheric Variables on an APE

Except for SM, some atmospheric factors, such as CAPE, MSE, LTS, WSR, and MFD, were also found to affect afternoon precipitation. Among these variables (Figure 7), $APE_{1\text{hour}}$ is more closely related to CAPE and MSE ($r = 0.24$ and 0.27 , respectively). LHFA and WSR have opposite effects on $APE_{1\text{hour}}$ ($r = 0.17$ and -0.15 , respectively). Meanwhile, atmospheric variables, such as LHFA, SHFA, CAPE, MSE, and LTS, are more associated with SMA (Figure 7). To diagnose the roles of these factors in an APE, we further analyzed the joint effect of SMA and these atmospheric variables introduced in Section 2. Since we focus on conditions prior to the onset of an APE, mean values of SMA and these atmospheric variables in the morning corresponding to an APE were calculated. They were then divided into five groups of equal size, and the mean $APE_{1\text{hour}}$ and precipitation frequency of an APE in each group were calculated.

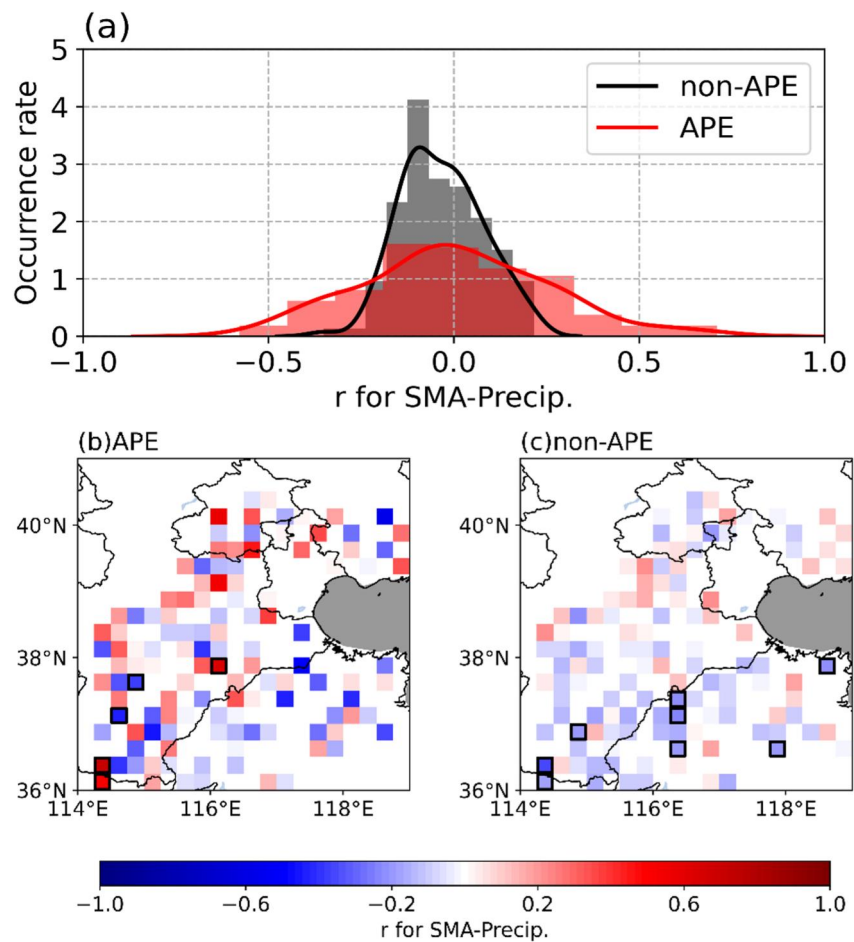


Figure 5. (a) Probability distribution of the correlation coefficient (r) for soil moisture anomaly (SMA) and precipitation amount in the first hour of afternoon precipitation event ($\text{APE}_{1\text{hour}}$) and $\text{non-APE}_{1\text{hour}}$ on each grid. (b) and (c) are the spatial distributions of r in the North China Plain for APE and non-APE. Black-bordered box on the grid point denotes the values of statistical significance ($p < 0.05$).

Figure 8a shows that APEs usually occur when MFD is negative, which means that moisture flux convergence benefits the formation of precipitation. The precipitation amount tends to be larger when WSR becomes small (Figure 8b), consistent with the finding of Findell and Eltahir (2003a) that strong wind shear inhibits convection and the coupling strength. Strong wind shear is not conducive to the development of convection, resulting in little moisture transported vertically, so the precipitation amount is smaller. A previous study revealed that LTS and SM are two key variables controlling cloud formation, hence precipitation over land (Wetzel et al., 1996). Figure 8c shows that $\text{APE}_{1\text{hour}}$ is larger when SMA is positive and when LTS is relatively high. MSE and CAPE are the two dominant factors for $\text{APE}_{1\text{hour}}$ (Figures 8d and 8e). Under high MSE or CAPE conditions, $\text{APE}_{1\text{hour}}$ is always large. These conclusions can also be drawn from Figure 9 which is calculated using SMA from GLDAS.

From the perspective of the APE occurrence frequency (Figure 8), an APE is found to occur over wetter (drier) soil when LTS, CAPE, or MSE is high (low). These results are more significant when using SMA from GLDAS than in-situ observations (Figure 9), partly because the GLDAS data set has sufficient samples and less uncertainties. Moreover, probability distributions of atmospheric variables under different SM conditions clearly show that atmospheric variables, such as LHFA, LTS, CAPE, and MSE, are smaller (larger), but SHFA is larger (smaller) over drier (wetter) soil when an APE happens (Figures S5 and S6 in Supporting Information S1). These results align with the findings of a coupled LES and land surface model (Huang & Margulis, 2011) and a single-column model (Ek & Holtlag, 2004). When LTS is weak, the growth of the boundary layer is less restricted, and a

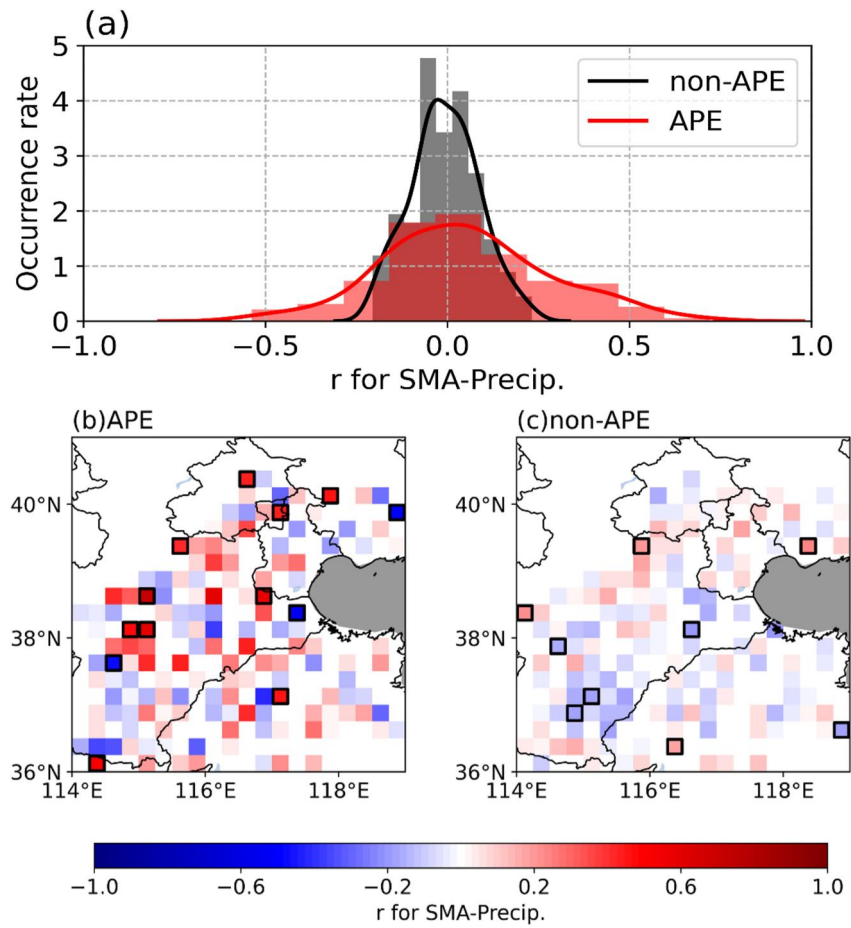


Figure 6. Similar to Figure 5, but using soil moisture data from Global Land Data Assimilation System.

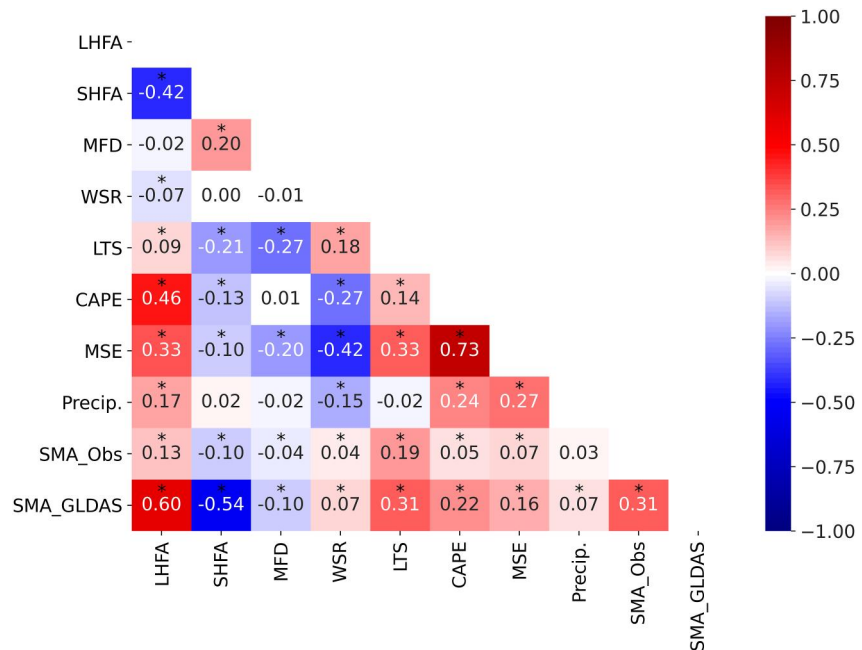


Figure 7. Correlation coefficients among atmospheric variables under afternoon precipitation event (APE) conditions, where the stars indicate that the values are statistically significant ($p < 0.05$).

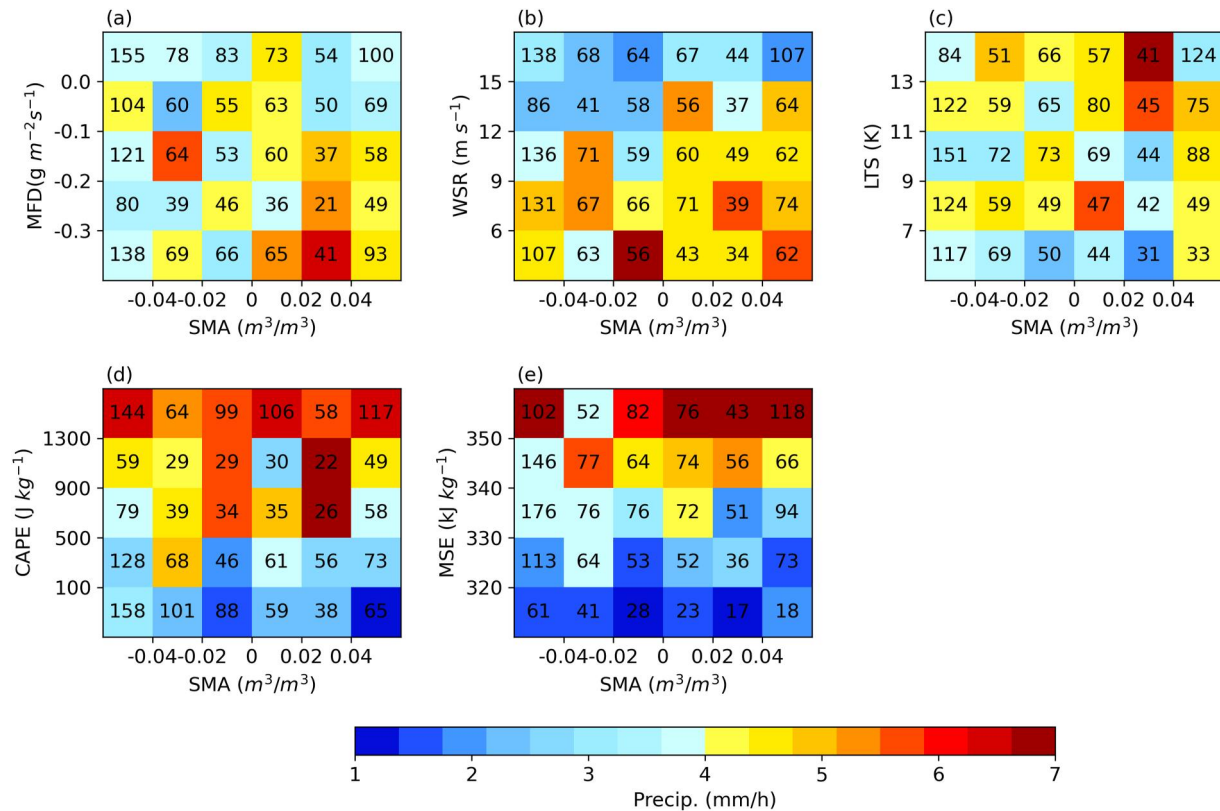


Figure 8. The joint distributions of soil moisture anomaly and atmospheric variables (a) moisture flux divergence, (b) vertical shear of horizontal wind (WSR), (c) low-tropospheric stability (LTS), (d) moist static energy, (e) convective available potential energy on the precipitation amount in the first hour of afternoon precipitation event (APE_{1hour}) (color shaded grid). The number in each grid means the number of APE.

stronger vertical motion associated with larger SHF over drier soils brings water vapor to the LCL, increasing the relative humidity at the top of the boundary layer and thus the possibility of cloud cover and precipitation (Huang & Margulis, 2011). Under higher LTS conditions, the lower troposphere is more stable, resulting in a shallower boundary layer. Wet soil moistens the boundary layer via increased LHF, thereby increasing the potential for cloud development and subsequent precipitation amount and frequency. In addition to tropospheric stability, tropospheric moisture and temperature are also crucial to the variation of relative humidity at the top of the boundary layer. Wetter soil favors active convection in a wet atmosphere (i.e., high CAPE and MSE) and strong tropospheric stability directly through moistening the boundary layer and indirectly through less entrainment (Gentine et al., 2013). Warmer tropospheric conditions with weak stratification favor active convection over dry soil (Gentine et al., 2013).

4. Conclusions

The impact of antecedent SM on subsequent precipitation is still debatable, with findings at odds among different study regions and investigation methods. In this study, the relationship between morning SM and afternoon precipitation on a sub-daily timescale during the warm seasons (May–September) of 2010–2019 was comprehensively investigated over the NCP, where land-atmosphere coupling is strongest in China. We found that the SM anomaly (SMA) has impacts on APEs, mainly by affecting the frequency of the onset of rainfall and to a lesser degree, affecting the precipitation amount of an APE. An APE tends to occur over drier soil with lower LTS, CAPE, or MSE. Under conditions of higher LTS, CAPE, or MSE, an APE tends to occur over wetter soil.

The SMA mainly controls the frequency of an APE. Once an APE occurs, the precipitation amount associated with the APE is almost independent of the SMA. A study focused on the eastern United States and Mexico also shows that the afternoon precipitation frequency, rather than precipitation amount, is correlated with the pre-noon evaporative fraction (Findell et al., 2011). There is a positive correlation in the eastern United States and most

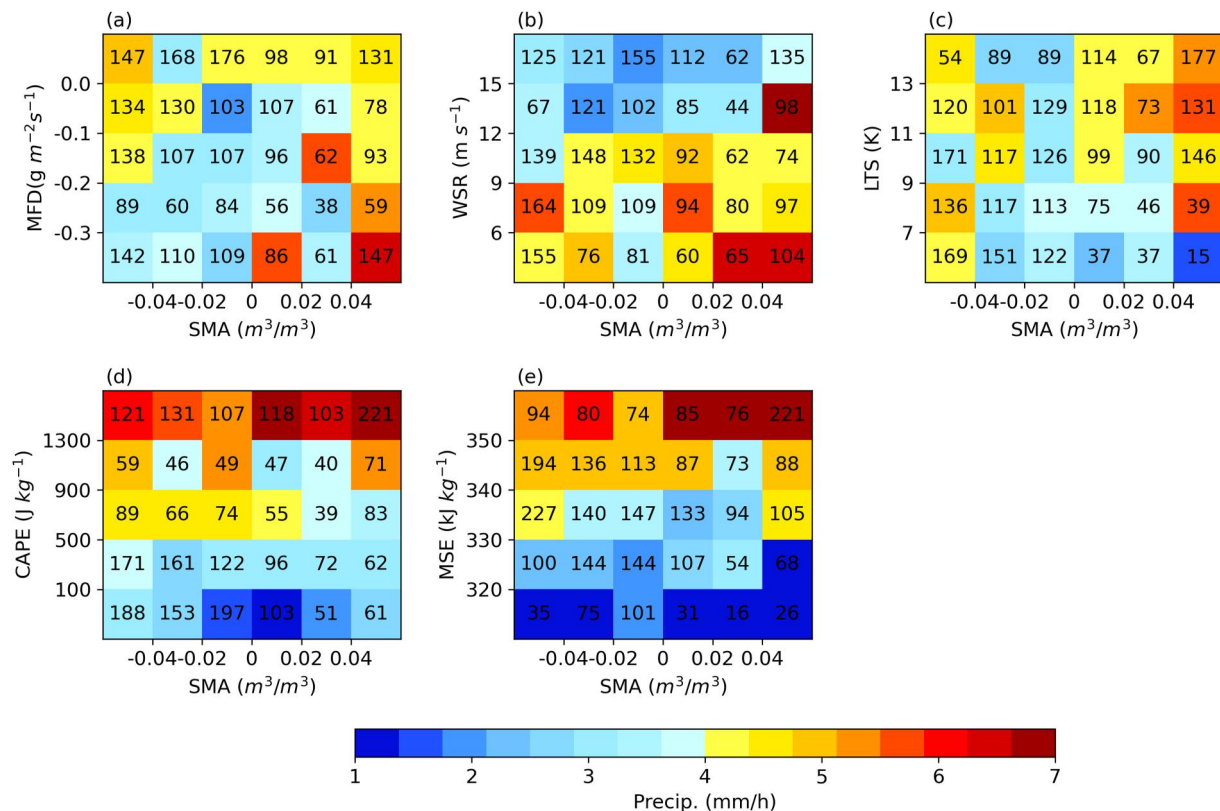


Figure 9. Same as Figure 8, but using soil moisture data from Global Land Data Assimilation System.

parts of the world (Findell et al., 2011; Guillod et al., 2015). However, we found a negative correlation in the NCP. These opposing results may be due to prevailing atmospheric conditions in these two different regions. Although in-situ measurements indicate ambiguity between accumulated precipitation in the first hour of APE (APE_{1hour}) and SMA, analyses with data from the GLDAS show a positive correlation between SMA and APE_{1hour} in the NCP. The possible mechanism is that increasing LHF over wetter soil leads to greater APE_{1hour} .

The joint effect of the SMA and atmospheric variables on an APE was also examined. Wetter soil under wet atmospheric conditions increases the potential for cloud development and subsequent precipitation, mainly through moistening the boundary layer via increased LHF and less entrainment. Drier soil under dry atmospheric conditions benefits the development of clouds and precipitation, mainly through thermodynamics associated with larger sensible heat fluxes, which brings water vapor to the LCL. These two mechanisms increase the relative humidity at the top of the boundary layer, increasing the possibility of cloud cover and precipitation.

We examined the relationship between morning SM and APEs based on statistical methods. Process-level mechanisms should be further investigated using radiosonde data, which would provide a detailed characterization of the vertical distribution of atmospheric parameters.

Data Availability Statement

The in-situ SM data and precipitation data are provided by the China Meteorological Data Service Centre, China Meteorological Administration (CMA, 2019). ERA5 data are provided by the ECMWF (ERA5, 2019; Hersbach et al., 2020). GLDAS data (Rodell et al., 2004) can be downloaded from NASA Goddard Earth Sciences Data and Information Services Center (GES DISC).

References

Brockhaus, P., Hohenegger, C., Bretherton, C. S., & Schär, C. (2009). The soil moisture–precipitation feedback in simulations with explicit and parameterized convection. *Journal of Climate*, 22(19), 5003–5020. <https://doi.org/10.1175/2009jcli2604.1>

Acknowledgments

This research is supported by the National Natural Science Foundation of China (42030606, 42325501, and U2142209). Besides, the authors are grateful to the anonymous reviewers and editors for their constructive comments.

- Carey, R. (1978). Atmospheric science: An introductory survey. *Physics Bulletin*, 29(6), 273–274. <https://doi.org/10.1088/0031-9112/29/6/037>
- Cioni, G., & Hohenegger, C. (2017). Effect of soil moisture on diurnal convection and precipitation in large-eddy simulations. *Journal of Hydrometeorology*, 18(7), 1885–1903. <https://doi.org/10.1175/jhm-d-16-0241.1>
- CMA. (2019). Meteorological data [Dataset]. *China Meteorological Administration*. Retrieved from <http://data.cma.cn/>
- Cook, B. I., Bonan, G. B., & Levis, S. (2006). Soil moisture feedbacks to precipitation in Southern Africa. *Journal of Climate*, 19(17), 4198–4206. <https://doi.org/10.1175/JCLI3856.1>
- Dirmeyer, P. A. (2000). Using a global soil wetness dataset to improve seasonal climate simulation. *Journal of Climate*, 13(16), 2900–2922. [https://doi.org/10.1175/1520-0442\(2000\)013<2900:UAGSWD>2.0.CO;2](https://doi.org/10.1175/1520-0442(2000)013<2900:UAGSWD>2.0.CO;2)
- Dirmeyer, P. A. (2011). The terrestrial segment of soil moisture-climate coupling. *Geophysical Research Letters*, 38(16). <https://doi.org/10.1029/2011gl048268>
- Dirmeyer, P. A., & Chen, L. (2017). Impacts of land-use/land-cover change on afternoon precipitation over North America. *Journal of Climate*, 30(6), 2121–2140. <https://doi.org/10.1175/jcli-d-16-0589.1>
- Dirmeyer, P. A., Wang, Z., Mbuh, M. J., & Norton, H. E. (2014). Intensified land surface control on boundary layer growth in a changing climate. *Geophysical Research Letters*, 41(4), 1290–1294. <https://doi.org/10.1002/2013gl058826>
- Ek, M. B., & Holtslag, A. A. M. (2004). Influence of soil moisture on boundary layer cloud development. *Journal of Hydrometeorology*, 5(1), 86–99. [https://doi.org/10.1175/1525-7541\(2004\)005<0086:IOSMOB>2.0.CO;2](https://doi.org/10.1175/1525-7541(2004)005<0086:IOSMOB>2.0.CO;2)
- Eltahir, E. A. B. (1998). A soil moisture-rainfall feedback mechanism: 1. Theory and observations. *Water Resources Research*, 34(4), 765–776. <https://doi.org/10.1029/97wr03499>
- ERA5. (2019). ERA5 hourly data on single levels from 1940 to present [Dataset]. *Copernicus/ECMWF*. Retrieved from <https://cds.climate.copernicus.eu/cdsapp#!/dataset/reanalysis-era5-single-levels?tab=overview>
- Fan, K., Zhang, Q., Singh, V. P., Sun, P., Song, C., Zhu, X., et al. (2019). Spatiotemporal impact of soil moisture on air temperature across the Tibet Plateau. *Science of the Total Environment*, 649, 1338–1348. <https://doi.org/10.1016/j.scitotenv.2018.08.399>
- Ferguson, C. R., Wood, E. F., & Vinukollu, R. K. (2012). A global intercomparison of modeled and observed land-atmosphere coupling. *Journal of Hydrometeorology*, 13(3), 749–784. <https://doi.org/10.1175/jhm-d-11-01119.1>
- Findell, K. L., & Eltahir, E. A. B. (2003a). Atmospheric controls on soil moisture-boundary layer interactions. Part I: Framework development. *Journal of Hydrometeorology*, 4(3), 552–569. [https://doi.org/10.1175/1525-7541\(2003\)004<0552:ACOSML>2.0.CO;2](https://doi.org/10.1175/1525-7541(2003)004<0552:ACOSML>2.0.CO;2)
- Findell, K. L., & Eltahir, E. A. B. (2003b). Atmospheric controls on soil moisture-boundary layer interactions. Part II: Feedbacks within the continental United States. *Journal of Hydrometeorology*, 4(3), 570–583. [https://doi.org/10.1175/1525-7541\(2003\)004<0570:ACOSML>2.0.CO;2](https://doi.org/10.1175/1525-7541(2003)004<0570:ACOSML>2.0.CO;2)
- Findell, K. L., Gentine, P., Lintner, B. R., & Kerr, C. (2011). Probability of afternoon precipitation in eastern United States and Mexico enhanced by high evaporation. *Nature Geoscience*, 4(7), 434–439. <https://doi.org/10.1038/ngeo1174>
- Gao, C., Chen, H., Sun, S., Xu, B., Ongoma, V., Zhu, S., et al. (2018). Regional features and seasonality of land-atmosphere coupling over eastern China. *Advances in Atmospheric Sciences*, 35(6), 689–701. <https://doi.org/10.1007/s00376-017-7140-0>
- Gao, Y., Hsu, P.-C., Che, S., Yu, C., & Han, S. (2022). Origins of intraseasonal precipitation variability over North China in the rainy season. *Journal of Climate*, 35(18), 6219–6236. <https://doi.org/10.1175/jcli-d-21-0832.1>
- Gentine, P., Holtslag, A. A. M., D'Andrea, F., & Ek, M. (2013). Surface and atmospheric controls on the onset of moist convection over land. *Journal of Hydrometeorology*, 14(5), 1443–1462. <https://doi.org/10.1175/jhm-d-12-0137.1>
- Guilford, B. P., Orlowsky, B., Miralles, D., Teuling, A. J., Blanken, P. D., Buchmann, N., et al. (2014). Land-surface controls on afternoon precipitation diagnosed from observational data: Uncertainties and confounding factors. *Atmospheric Chemistry and Physics*, 14(16), 8343–8367. <https://doi.org/10.5194/acp-14-8343-2014>
- Guilford, B. P., Orlowsky, B., Miralles, D. G., Teuling, A. J., & Seneviratne, S. I. (2015). Reconciling spatial and temporal soil moisture effects on afternoon rainfall. *Nature Communications*, 6(1), 6443. <https://doi.org/10.1038/ncomms7443>
- Guo, J., Su, T., Chen, D., Wang, J., Li, Z., Lv, Y., et al. (2019). Declining summertime local-scale precipitation frequency over China and the United States, 1981–2012: The disparate roles of aerosols. *Geophysical Research Letters*, 46(22), 13281–13289. <https://doi.org/10.1029/2019GL085442>
- Guo, J., Su, T., Li, Z., Miao, Y., Li, J., Liu, H., et al. (2017). Declining frequency of summertime local-scale precipitation over eastern China from 1970 to 2010 and its potential link to aerosols. *Geophysical Research Letters*, 44(11), 5700–5708. <https://doi.org/10.1002/2017gl073533>
- Guo, Z., Dirmeyer, P. A., Koster, R. D., Bonan, G., Chan, E., Cox, P., et al. (2006). GLACE: The global land-atmosphere coupling experiment. Part II: Analysis. *Journal of Hydrometeorology*, 7(4), 611–625. <https://doi.org/10.1175/JHM511.1>
- Hersbach, H., Bell, B., Berrisford, P., Hirahara, S., Horányi, A., Muñoz-Sabater, J., et al. (2020). The ERA5 global reanalysis. *Quarterly Journal of the Royal Meteorological Society*, 146(730), 1999–2049. <https://doi.org/10.1002/qj.3803>
- Holgate, C. M., Van Dijk, A. I. J. M., Evans, J. P., & Pitman, A. J. (2019). The importance of the one-dimensional assumption in soil moisture - rainfall depth correlation at varying spatial scales. *Journal of Geophysical Research: Atmospheres*, 124(6), 2964–2975. <https://doi.org/10.1029/2018jd029762>
- Hu, K., Xie, S.-P., & Huang, G. (2017). Orographically anchored El Niño effect on summer rainfall in Central China. *Journal of Climate*, 30(24), 10037–10045. <https://doi.org/10.1175/JCLI-D-17-0312.1>
- Huang, H.-Y., & Margulis, S. A. (2011). Investigating the impact of soil moisture and atmospheric stability on cloud development and distribution using a coupled large-eddy simulation and land surface model. *Journal of Hydrometeorology*, 12(5), 787–804. <https://doi.org/10.1175/2011jhm1315.1>
- Huang, M., Qian, Y., Yang, B., & Berg, L. K. (2013). A modeling study of irrigation effects on surface fluxes and land-air-cloud interactions in the Southern Great Plains. *Journal of Hydrometeorology*, 14(3), 700–721. <https://doi.org/10.1175/jhm-d-12-0134.1>
- Kang, S. L. (2016). Regional Bowen ratio controls on afternoon moist convection: A large eddy simulation study. *Journal of Geophysical Research: Atmospheres*, 121(23). <https://doi.org/10.1002/2016jd025567>
- Klein, S. A., & Hartmann, D. L. (1993). The seasonal cycle of low stratiform clouds. *Journal of Climate*, 6(8), 1587–1606. [https://doi.org/10.1175/1520-0442\(1993\)006<1587:TSCOLS>2.0.CO;2](https://doi.org/10.1175/1520-0442(1993)006<1587:TSCOLS>2.0.CO;2)
- Koster, R. D., Dirmeyer, P. A., Guo, Z., Bonan, G., Chan, E., Cox, P., et al. (2004). Regions of strong coupling between soil moisture and precipitation. *Science*, 305(5687), 1138–1140. <https://doi.org/10.1126/science.1100217>
- Li, D., & Wang, C. (2016). The relation between soil moisture over the Tibetan Plateau in spring and summer precipitation in the eastern China. *Journal of Glaciology and Geocryology*, 38(1), 89–99. <https://doi.org/10.7522/j.issn.10.0240.2016.0010>
- Li, M., Ma, Z., Gu, H., Yang, Q., & Zheng, Z. (2017). Production of a combined land surface data set and its use to assess land-atmosphere coupling in China. *Journal of Geophysical Research: Atmospheres*, 122(2), 948–965. <https://doi.org/10.1002/2016jd025511>

- Liang, L., & Chen, H. (2010). Possible linkage between spring soil moisture anomalies over South China and summer rainfall in China. *Transactions of Atmospheric Sciences*, 33, 536–546.
- Liu, L., Zhang, R., & Zuo, Z. (2017). Effect of spring precipitation on summer precipitation in eastern China: Role of soil moisture. *Journal of Climate*, 30(22), 9183–9194. <https://doi.org/10.1175/jcli-d-17-0028.1>
- Ma, Z., Wei, H., & Fu, C. (2000). Relationship between regional soil moisture variation and climatic variability over east China. *Acta Meteorologica Sinica*(3), 278–287. <https://doi.org/10.11676/qxxb2000.029>
- Milovac, J., Warrach-Sagi, K., Behrendt, A., Späth, F., Ingwersen, J., & Wulfmeyer, V. (2016). Investigation of PBL schemes combining the WRF model simulations with scanning water vapor differential absorption lidar measurements. *Journal of Geophysical Research: Atmospheres*, 121(2), 624–649. <https://doi.org/10.1002/2015jd023927>
- Müller, O. V., Vidale, P. L., Vannière, B., Schiemann, R., Senan, R., Haarsma, R. J., & Jungclaus, J. H. (2021). Land–atmosphere coupling sensitivity to GCMs resolution: A multimodel assessment of local and remote processes in the Sahel hot spot. *Journal of Climate*, 34(3), 967–985. <https://doi.org/10.1175/jcli-d-20-0303.1>
- Nicholson, S. E. (2015). Evolution and current state of our understanding of the role played in the climate system by land surface processes in semi-arid regions. *Global and Planetary Change*, 133, 201–222. <https://doi.org/10.1016/j.gloplacha.2015.08.010>
- Petrova, I. Y., van Heerwaarden, C. C., Hohenegger, C., & Guichard, F. (2018). Regional co-variability of spatial and temporal soil moisture–precipitation coupling in North Africa: An observational perspective. *Hydrology and Earth System Sciences*, 22(6), 3275–3294. <https://doi.org/10.5194/hess-22-3275-2018>
- Rodell, M., Houser, P. R., Jambor, U., Gottschalk, J., Mitchell, K., Meng, C.-J., et al. (2004). The global land data assimilation system [Dataset]. *Bulletin of the American Meteorological Society*, 85(3), 381–394. <https://doi.org/10.1175/BAMS-85-3-381>
- Santanello, J. A., Dirmeyer, P. A., Ferguson, C. R., Findell, K. L., Tawfik, A. B., Berg, A., et al. (2018). Land–atmosphere interactions: The LoCo perspective. *Bulletin of the American Meteorological Society*, 99(6), 1253–1272. <https://doi.org/10.1175/bams-d-17-0001.1>
- Seneviratne, S. I., Corti, T., Davin, E. L., Hirschi, M., Jaeger, E. B., Lehner, I., et al. (2010). Investigating soil moisture–climate interactions in a changing climate: A review. *Earth-Science Reviews*, 99(3–4), 125–161. <https://doi.org/10.1016/j.earscirev.2010.02.004>
- Song, Y., & Wei, J. (2021). Diurnal cycle of summer precipitation over the North China Plain and associated land–atmosphere interactions: Evaluation of ERA5 and MERRA-2. *International Journal of Climatology*, 41(13), 6031–6046. <https://doi.org/10.1002/joc.7166>
- Su, T., Li, Z., & Zheng, Y. (2023). Cloud-surface coupling alters the morning transition from stable to unstable boundary layer. *Geophysical Research Letters*, 50(5), e2022GL102256. <https://doi.org/10.1029/2022gl102256>
- Su, T., Zheng, Y., & Li, Z. (2022). Methodology to determine the coupling of continental clouds with surface and boundary layer height under cloudy conditions from lidar and meteorological data. *Atmospheric Chemistry and Physics*, 22(2), 1453–1466. <https://doi.org/10.5194/acp-22-1453-2022>
- Talib, J., Müller, O. V., Barton, E. J., Taylor, C. M., & Vidale, P. L. (2023). The representation of soil moisture–atmosphere feedbacks across the Tibetan Plateau in CMIP6. *Advances in Atmospheric Sciences*, 40(11), 2063–2081. <https://doi.org/10.1007/s00376-023-2296-2>
- Tawfik, A. B., & Dirmeyer, P. A. (2014). A process-based framework for quantifying the atmospheric preconditioning of surface-triggered convection. *Geophysical Research Letters*, 41(1), 173–178. <https://doi.org/10.1002/2013gl057984>
- Taylor, C. M. (2015). Detecting soil moisture impacts on convective initiation in Europe. *Geophysical Research Letters*, 42(11), 4631–4638. <https://doi.org/10.1002/2015gl064030>
- Taylor, C. M., de Jeu, R. A. M., Guichard, F., Harris, P. P., & Dorigo, W. A. (2012). Afternoon rain more likely over drier soils. *Nature*, 489(7416), 423–426. <https://doi.org/10.1038/nature11377>
- Taylor, C. M., Gounou, A., Guichard, F., Harris, P. P., Ellis, R. J., Couvreur, F., & De Kauwe, M. (2011). Frequency of Sahelian storm initiation enhanced over mesoscale soil-moisture patterns. *Nature Geoscience*, 4(7), 430–433. <https://doi.org/10.1038/ngeo1173>
- Tian, J., Zhang, Y., Guo, J., Zhang, X., Ma, N., Wei, H., & Tang, Z. (2022). Predicting root zone soil moisture using observations at 2121 sites across China. *Science of the Total Environment*, 847, 157425. <https://doi.org/10.1016/j.scitotenv.2022.157425>
- Tong, B., Guo, J., Xu, H., Wang, Y., Li, H., Bian, L., et al. (2022). Effects of soil moisture, net radiation, and atmospheric vapor pressure deficit on surface evaporation fraction at a semi-arid grass site. *Science of the Total Environment*, 849, 157890. <https://doi.org/10.1016/j.scitotenv.2022.157890>
- Wang, A., Kong, X., Chen, Y., & Ma, X. (2022). Evaluation of soil moisture in CMIP6 multimodel simulations over conterminous China. *Journal of Geophysical Research: Atmospheres*, 127(19). <https://doi.org/10.1029/2022jd037072>
- Wei, J., & Dirmeyer, P. A. (2012). Dissecting soil moisture–precipitation coupling. *Geophysical Research Letters*, 39(19), L19711. <https://doi.org/10.1029/2012gl053038>
- Welty, J., Stillman, S., Zeng, X., & Santanello, J. (2020). Increased likelihood of appreciable afternoon rainfall over wetter or drier soils dependent upon atmospheric dynamic influence. *Geophysical Research Letters*, 47(11). <https://doi.org/10.1029/2020gl087779>
- Welty, J., & Zeng, X. (2018). Does soil moisture affect warm season precipitation over the Southern Great Plains? *Geophysical Research Letters*, 45(15), 7866–7873. <https://doi.org/10.1029/2018gl078598>
- Wetzel, P. J., Argentini, S., & Boone, A. (1996). Role of land surface in controlling daytime cloud amount: Two case studies in the GCIP-SW area. *Journal of Geophysical Research*, 101(D3), 7359–7370. <https://doi.org/10.1029/95jd02134>
- Wu, R. (2016). Relationship between Indian and east Asian summer rainfall variations. *Advances in Atmospheric Sciences*, 34(1), 4–15. <https://doi.org/10.1007/s00376-016-6216-6>
- Wu, Y., Li, P., & Chen, H. (2023). The characteristic and seasonal variation of mesoscale convective systems' precipitation over North China. *Quarterly Journal of the Royal Meteorological Society*, 149(755), 2348–2366. <https://doi.org/10.1002/qj.4510>
- Xia, Y., Sheffield, J., Ek, M. B., Dong, J., Chaney, N., Wei, H., et al. (2014). Evaluation of multi-model simulated soil moisture in NLDAS-2. *Journal of Hydrology*, 512, 107–125. <https://doi.org/10.1016/j.jhydrol.2014.02.027>
- Zhang, J., Guo, J., Li, J., Shao, J., Tong, B., & Zhang, S. (2022). The prestorm environment and prediction for local- and nonlocal-scale precipitation: Insights gained from high-resolution radiosonde measurements across China. *Journal of Geophysical Research: Atmospheres*, 127(18). <https://doi.org/10.1029/2021jd036395>
- Zhang, X., Wang, Y. P., & Zhang, Y. (2023). Strong nonlinearity of land climate-carbon cycle feedback under a high CO₂ growth scenario. *Earth's Future*, 11(1). <https://doi.org/10.1029/2021ef002499>
- Zhao, C., Meng, X., Li, Y., Lyu, S., Guo, J., & Liu, H. (2022). Impact of soil moisture on afternoon convection triggering over the Tibetan Plateau based on 1-D boundary layer model. *Journal of Geophysical Research: Atmospheres*, 127(2). <https://doi.org/10.1029/2021jd035591>
- Zhong, S., Yang, T., Qian, Y., Zhu, J., & Wu, F. (2018). Temporal and spatial variations of soil moisture – Precipitation feedback in East China during the East Asian summer monsoon period: A sensitivity study. *Atmospheric Research*, 213, 163–172. <https://doi.org/10.1016/j.atmosres.2018.05.014>

- Zhu, C., Ullah, W., Wang, G., Lu, J., Li, S., Feng, A., et al. (2023). Diagnosing potential impacts of Tibetan Plateau spring soil moisture anomalies on summer precipitation and floods in the Yangtze River Basin. *Journal of Geophysical Research: Atmospheres*, *128*(8). <https://doi.org/10.1029/2022jd037671>
- Zuo, Z., & Zhang, R. (2007). The spring soil moisture and the summer rainfall in eastern China. *Chinese Science Bulletin*, *52*(23), 3310–3312. <https://doi.org/10.1007/s11434-007-0442-3>
- Zuo, Z., & Zhang, R. (2011). Impact of spring soil moisture on surface energy balance and summer monsoon circulation over east Asia and precipitation in east China. *Journal of Climate*, *24*(13), 3309–3322. <https://doi.org/10.1175/2011jcli4084.1>